Alexandria Engineering Journal (2014) 53, 903–910

HOSTED BY

Alexandria University

Alexandria Engineering Journal

www.elsevier.com/locate/aej
www.sciencedirect.com

Performance of footing with single side micro-piles adjacent to slopes

Ahmed Elzoghby Elsaied *,[1]

Construction Research Institute, Egypt

Received 22 February 2014; revised 1 July 2014; accepted 14 July 2014
Available online 12 August 2014

KEYWORDS

Micro-piles;
Strip footing;
Slope stability;
Bearing capacity;
Sand

Abstract This research was initiated in order to investigate the capability of rigid strip one side micro-piles footings in stabilizing sand slopes. A physical model was designed and constructed for micro-piles footings resting on dense sand. Measuring devices were arranged; load-settlement measurements of the model footings were recorded; photos were captured and observations were documented. Different footing configurations located at variable distances from slope edge were tested; five groups of micro-piles depths were inspected and different eccentric vertical so as oblique loads were examined to investigate its capability of stabilizing the slopes. Measurements were plotted and analyzed. Comparison was carried out among the inspected cases. Results indicated that a significant enhancement to the bearing capacity of single side micro-piles footing was documented with the increase of micro-piles depth. It reached about 7.9 times that of footing without micro-piles.

1. Introduction

In terms of the importance of stabilizing the slopes, different techniques are available. Micro-piles are one of the most economical solutions for improving footing behavior nearby slopes. Footings might be located on/or nearby slopes according to the architectural requirements or according to the permitted space such as bridge abutments, retaining walls, foundations next to excavations and foundations built on mountain slopes [1]. Also, cost savings might be achieved if the footing is located as close as possible to the edge of the slope with keeping it as steep as possible. Therefore; this research was initiated in order to perceive a better understanding to use the micro-piles on slopes.

2. Literature review

Literature in the field of micro piles was revised. From the literature, it was stated that there are several theoretical methods for predicting the bearing capacity of shallow footings located in or on the top surface of a slope. Some of these bearing capacity theories are based on the method of stress characteristics [2] and others are based on limit equilibrium and limit analysis approaches [3,4]. Based on experimental data it was reported that the ultimate bearing capacity is reduced as the footing get closer to the slope crest [5–7]. Based on the

* Tel.: +20 10 0188 65 97.
E-mail address: zog1969@yahoo.com.
[1] Researcher in construction research institute, Egypt.
Peer review under responsibility of Faculty of Engineering, Alexandria University.

http://dx.doi.org/10.1016/j.aej.2014.07.004
1110-0168

literature, it was documented that several researchers conducted laboratory-model scaled centrifuge tests for shallow foundations located on or nearby slopes [8]. A Full-scale field test was carried for investigating the bearing capacity of inclined footing with anchors on granular slopes [9]. Generally the bearing capacity decreases with an increase in slope angle as well as a decrease in the distance between the footing edge and the slope crest.

These theories gave widely varying answers for identical footing locations and same soil conditions. Moreover; all of the above mentioned analytical and experimental works assumed that the load was vertically applied and was concentric to the footing base which is far from reality. However, for most practical cases, the resultant load acts on the footing with a certain inclination and sometimes with certain eccentricity [10,11]. Moreover, the load bearing capacity of shallow foundations located on sand slopes can be improved by reinforcement or stabilization. Experimental work in this area of research was carried out for a reinforced sandy slope [12,13].

3. Micro-piles

Micro-piles can be installed in a variety of challenging subsurface conditions. They provided an improving resistance to driving forces resulting in a higher factor of safety. Micro-piles are installed using the same drilling and grouting equipment as used for the installation of tiebacks or soil nails. This approach is based on the use of "micro-piles" fixed to the edges of the footing. This method does not need a wide excavation of soil, and hence it is not restricted by the presence of high water tables.

Many studies were conducted to investigate the effectiveness of micro-piles installation on load transfer mechanisms and the deformation behavior of soil subjected to additional surface loading. The micro-piles effects on soil behavior were explained. The soil response under surface loading was significantly improved by micro-piles installation [14–16]. Tests on micro-piles were carried out [17–19].They concluded that the bearing capacity and stiffness of the subgrade reaction of soil were increased considerably and the ground settlement also was decreased. A design of micro-piles for tunnel face reinforcement was done [20]. The deviations in the research results might be attributed to the difference in the assumed rupture surface, lack of the evaluation process or underestimation of governing parameters especially that affecting soil bearing capacity. As a result, the foundation bearing capacities should be selected conservatively.

To date, literature lacks data on the behavior of micro-piles footing on or nearby slopes crest under different loading conditions represented a motivation to carry out the proposed research. This study improved the understanding behavior of this promising soil improvement technique. Also the available solutions for the bearing capacity problem of footings on slopes are based mostly on experimental considerations, and give widely varying answers for identical footing configuration and soil conditions.

4. Experimental work

An experimental physical model was designed and prepared. Measuring devices were arranged and experiments were executed. An experimental program was designed and different loading tests were conducted on the designed physical model.

4.1. Physical model

The physical model consists of a tank, footing of micro-piles, loading system and a settlement measuring device. The rigid steel tank has inner dimensions of $2000 \times 300 \times 800$ mm length, width, and depth, respectively. The tank consists of four sided perspex ply stiffened all around with rigid steel sections to allow for limited deformation during loading process. The footing model is prepared using a stiff steel plate $150 \times 12 \times 295$ mm width, thickness and length, respectively. The footing length with its longitudinal direction fits within the tank width with a 2.5 mm recess at both sides. Any deformation is prevented to occur along the footing longitudinal direction, which leads to achieve a plain strain condition throughout the tests. The base of footing was made to have a rough surface.

A vertical plate ($100 \times 50 \times 4$ mm) is welded at the top of the footing to provide reference for the dial gauge in lateral direction. The load is transmitted at the top of the footing through a loading ball of 16 mm diameter. The ball is fitted between the rigid bar and the footing. A recess from the center of the footing plate and at the required eccentricities is achieved. The recess to accommodate a ball bearing through which the loads were applied to the footing.

4.2. Designed experimental program

An experimental program was designed. It included five groups of high tensile steel bars with 20 mm diameter and with different heights. Each group contains five micro-piles with the same height. The depths of the micro-piles after fixation on the footing base were 75, 150, 300, 450, and 600 mm i.e. L/B = 0.5, 1.0, 2.0, 3.0 and 4.0, respectively. In order to ensure rigid fixation, between the micro-piles and the footing, five holes with the full footing depth were drilled at equal spacing of 60 mm in the specified position to support the micro-piles. Each hole was 20 mm diameter. The micro-piles were connected to the footing by steel bolts.

A rigid loading frame was used to apply the load to the model strip footing through hydraulic jack and 50 KN proving ring. Dial gauges were used to measure the footing movements. The details of the loading frame are indicated in Fig. 1. Fig. 2 presents the examined micro-piles and footing. A schematic diagram of this study is shown in Fig. 3.

Where:

B: Footing width.
e: Load eccentricity.
X: Distance of the footing edge to the slope crest.
L: Micro-piles length.
i: Load inclination angle.
θ: Slope inclination angle.

It is to be noted that a model strip footing with/without single side micro-piles tests on sand slopes was inspected at two slope angles of 2H: 1V (θ = 26.6°) and 3H: 2V (θ = 33.7°) with different footing edge distances from slope crest to the footing width ratio, X/B, of 0, 1.0, 2.0, 3.0, 4.0 and 5.0 for five

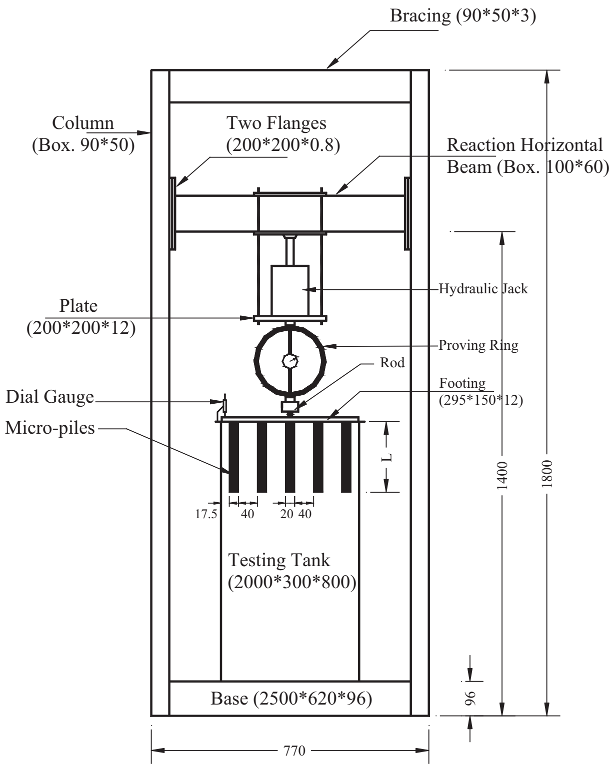

Figure 1 Model configuration (dimensions in mm).

Figure 2 The examined footing and micro-piles.

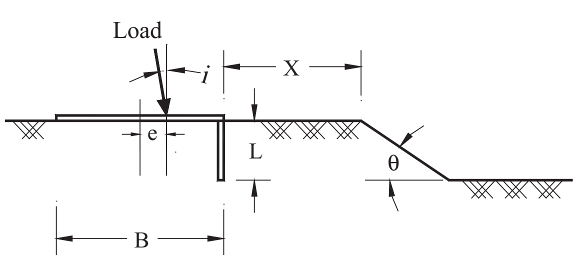

Figure 3 Schematic diagram showing experimental configuration.

groups of micro-piles depths as described above. Three different loading conditions were examined; vertical concentric, vertical eccentric and concentric oblique loading. The first series was concerned with micro-piles footing behavior under vertical loading. The second test series was performed under eccentric loading where e/B of 0.133 and 0.266 in the direction of the slope crest. The third series was carried out to investigate the effect of concentric oblique loading with inclination angle to the vertical ($i = 10°$) on the micro-piles footing system behavior.

For comparison purposes, a test on flat horizontal ground was conducted to provide the necessary reference data. Finally, a total number of 72 footings with/without micro-piles tests were carried out.

4.3. Implemented material

The implemented sand is dense and it is classified as poorly graded sand (SP) according to the Unified system. The grain size distribution is 45% coarse sand, 50% medium sand, and 5% fine sand. The sand has maximum dry density of 18.2 KN/m^3; minimum dry density of 15.7 KN/m^3 and specific gravity of 2.51. The sand was kept dry during model tests and the bulk density is 17.5 KN/m^3. All the model tests were conducted at a relative density of 75%, for which the friction angle from a direct shear test was found to be 38°.

4.4. Testing procedure

Different slope angles were prepared. Sand was compacted in 100 mm thick layers to fill the tank. The slope height of 300 mm was kept constant for all the tests to minimize the rigid boundary effect of the testing tank. The unit weight of sand and the required relative density were controlled by pouring a pre-calculated weight of sand into the testing tank, to fill each layer. The sand surface was leveled and compacted. Great care was taken to level the top surface of the sand and the slope face using special straight edge so that the relative density of the top layer does not change. Reference slope markers on the perspex walls were used to form the required slope inclination. The accuracy of the sand density inside the tank was checked by conducting three preliminary density tests. The variation in the sand relative density was found to be 75% ± 0.50%.

Regarding the test procedure:

- Joining the micro-piles to the guide beam using five screw bolts.
- Fixing the guide beam to the top angles of the tank sides using bolts and nuts.
- Fixing the micro-piles and placing them at the desired level from the top surface level of the compacted sand at the required location. This installation keeps the micro-piles in place during completing the sand filling around it.
- Continuing the sand filling process above the micro-piles till the top surface of the test tank.
- Removing the guide beam and fixing the model strip footing to the micro-piles. Installation details of the micro-piles procedures are described and are presented in Fig. 4.

(a) Fixing micro-piles on guide beam and complete sand formation

(b) Removing the guide beam

(c) Fixing the footing with micro-piles

Figure 4 Micro-piles installation procedure.

- Appling the load to the footing, at the required eccentricity and load inclination angle by slowly using the hydraulic jack. The rigid bar under the ring will touch the ball placed on the footing surface before "zero-reading" appears on the load ring.
- Mounting the dial gauges, for measuring the footing movements, on the tank. One gauge measure the vertical displacement while the second measures the horizontal displacement.
- After taking the zero-reading, the load is applied at small increments with a rate of 0.005 N/mm^2, until the failure of the foundation occurs. It is very important that a sufficient time is allowed after each increment. This time ranges from several seconds at early staged of loading to approximately 30 s as being close to failure. The failure is marked by a sudden considerable variation in the load-settlement curves.

5. Results analysis

Measurements were obtained, analyzed and plotted. A sample of the results is presented. The load-settlement curves of the experimental model tests of strip footing with/without single side micro-piles resting on the horizontal ground of sand slopes were obtained. The ultimate bearing capacity was determined from the load-settlement curves by using the point of failure. The obtained results were discussed to study the effect of different loading conditions centric/eccentric vertical load and centrically oblique load on the behavior of one side micro-piles footing as fallows.

5.1. Vertical loading

This series of tests studied the behavior of the strip footing with/without single side micro-piles under the effect of centrically vertical load. The strip footing behavior, without micro-piles, placed at various distances to the slope crest were determined. Also, the footing behavior with single side micro-piles placed at $X/B = 2.0$ from the slope crest was obtained. The micro-piles depth varied between zero and three times as the footing width.

Regarding the footing without micro-piles, the load-settlement curves of the experimental model strip footing without micro-piles are presented in Figs. 5 and 6. The test results indicated that the ultimate bearing capacity increased as the

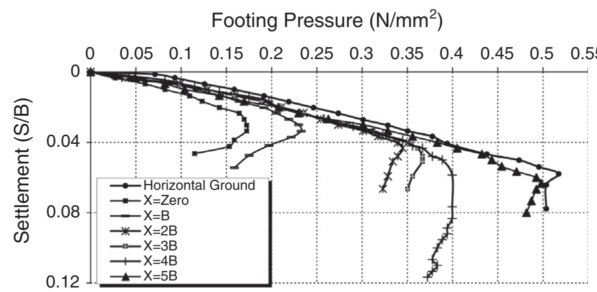

Figure 5 Load-settlement relations for concentric loaded footing (slope 2:1).

footing placed far from the slope crest as well as with the decrease in slope inclination angle.

For comparison purposes, the result for the case of horizontal ground surface was used as a reference. Increasing the footing edge distance, X/B, increased the footing bearing capacity in a trial to reach the same value of the reference footing on horizontal ground. Approximately the same behavior and trend was observed for the two different slope angles. This is due to the expected increase in the passive resistance from the slope side to the wedge of failure under the footing. Most of the bearing capacity increment takes place at a ratio of X/B of 0.0 and 2.0.

The experimental results were found in a good agreement with that proposed by [1,4]. They stated that the ultimate bearing capacity, for strip footing under vertical centric load, is not affected by slopes at X/B is equal to 4.0 and 5.0, respectively.

By comparing Figs. 5 and 6, the effect of slope angle on the bearing capacity is recognized. As expected, increasing the slope angle decreased the ultimate bearing capacity of the slope. This can be attributed to the decreased shearing resistance of the supporting soil near the slope face due to either the reduced slip line field or the decreased confinement effect resulting from increasing slope angle.

As for micro-piles footing, the load-settlement curves of single side micro-piles strip footing subjected to vertical centric loads are presented in Fig. 7. In these tests, the micro-piles depth varied from zero to three times the footing width. The micro-piles footing edge was placed at twice the footing width from the slope crest.

The results indicated that increasing the micro-piles depth up to $L = B$, leads to a decrease in the footing pressure, at

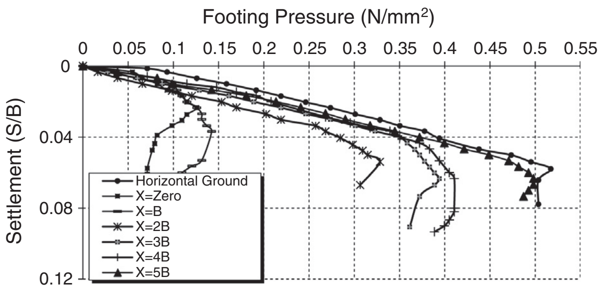

Figure 6 Load-settlement relations for concentric loaded footing (slope 3:2).

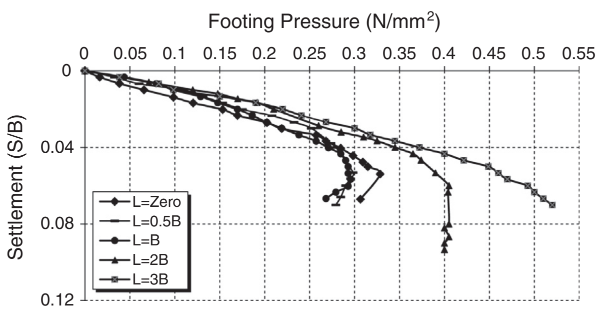

Figure 7 Load-settlement relations for vertical concentric loaded micro-piles footing at $X/B = 2.0$ (slope 3:2).

high stress near and beyond the failure load, compared to the case of strip footing without micro-piles. This is due to the fact that the micro-piles behave as a support to the footing from one edge only. As a result, the footing-micro-piles system rotates and the rotation increased with the increased of the micro-piles depth up to $L = B$.

Increasing the micro-piles embedment depth beyond $L = B$, increased the micro-piles interface area, which enhanced the footing behavior to resist rotation and sustain additional loading.

5.2. Eccentric loading

The behavior of single side micro-piles strip footing resting on sandy slope (3:2) was determined. The micro-piles strip footing was subjected to vertical eccentric load within and outside the footing middle third e/B ratio was selected 0.133 and 0.266. The effect of the footing position t o the slope crest and the footing behavior with various micro-piles depths were obtained.

Regarding the footing without micro-piles, the load-settlement relations of strip footing without micro-piles are plotted in Fig. 8. It is clearly indicated that, the bearing capacity proportionally increases as the footing edge distance "X/B" increases. The curves demonstrated that the larger the load eccentricity the less the soil bearing capacity. This was due to the fact that as the load eccentricity increased, the failure wedge beneath the footing got smaller and shallower. The expected increase in footing tilting due to load eccentricity forced the footing to lose some of its contact with soil. Moreover, the soil spread outward toward the slope face caused by the greater settlement in the footing edge nearer to loading than the other edge. Generally, footing eccentrically loaded

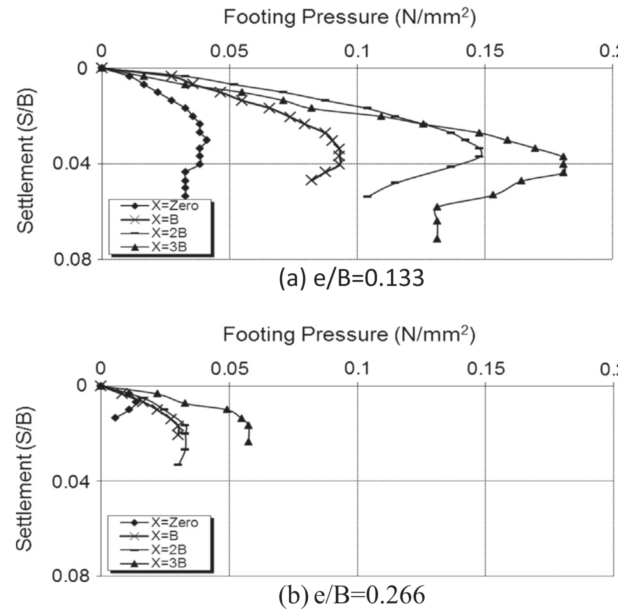

Figure 8 Load-settlement relations for vertical eccentric loaded footing on slope 3:2.

failed earlier than the concentrically vertical loaded footing due to tilting.

As for micro-piles footing, samples of the load-settlement relations of the experimental model micro-piles strip footing tests resting on the top of sand slopes are presented in Fig. 9. The results indicated a similar trend. Increasing the micro-piles depth, leads to an increase in the bearing capacity. This is due to the presence of micro-piles which decreased the subgrade deformation and prevented the soil particles under the footing from moving laterally. The micro-piles depth should be extended to a sufficient depth below the failure surface to get the most beneficial effect of the footing-micro-piles system. The optimum micro-piles depth is an important factor in the micro-piles footing design. The optimum depth value is controlled by different parameters such as footing depth, load inclination angle, soil density and gradation. The increase in the ultimate bearing capacity of micro-piles footing compared to footing without micro-piles can be expressed in terms of dimensionless parameter called the ultimate Bearing Capacity Ratio (BCR_u).

The bearing capacity ratio at ultimate load is defined as: $BCR_u = \frac{q'_{ult}}{q_{ult}}$
where

- q'_{ult}: ultimate bearing capacity of micro-piles footing.
- q_{ult}: ultimate bearing capacity of same footing without micro-piles.

The increase in the ultimate bearing capacity ratio BCR_u due to the usage of single side micro-piles footing subjected to vertical eccentric load is plotted in Fig. 10 for different micro-piles depths. The BCR_u increased with the increase in the micro-piles depth. It reached its maximum value at micro-piles depth equals to twice the footing width ($L/B = 2.0$). This is because the micro-piles depth is deep enough to reach the stable soil just beneath the slope bed. This was due to the micro-piles settled down the slope bed as a result of

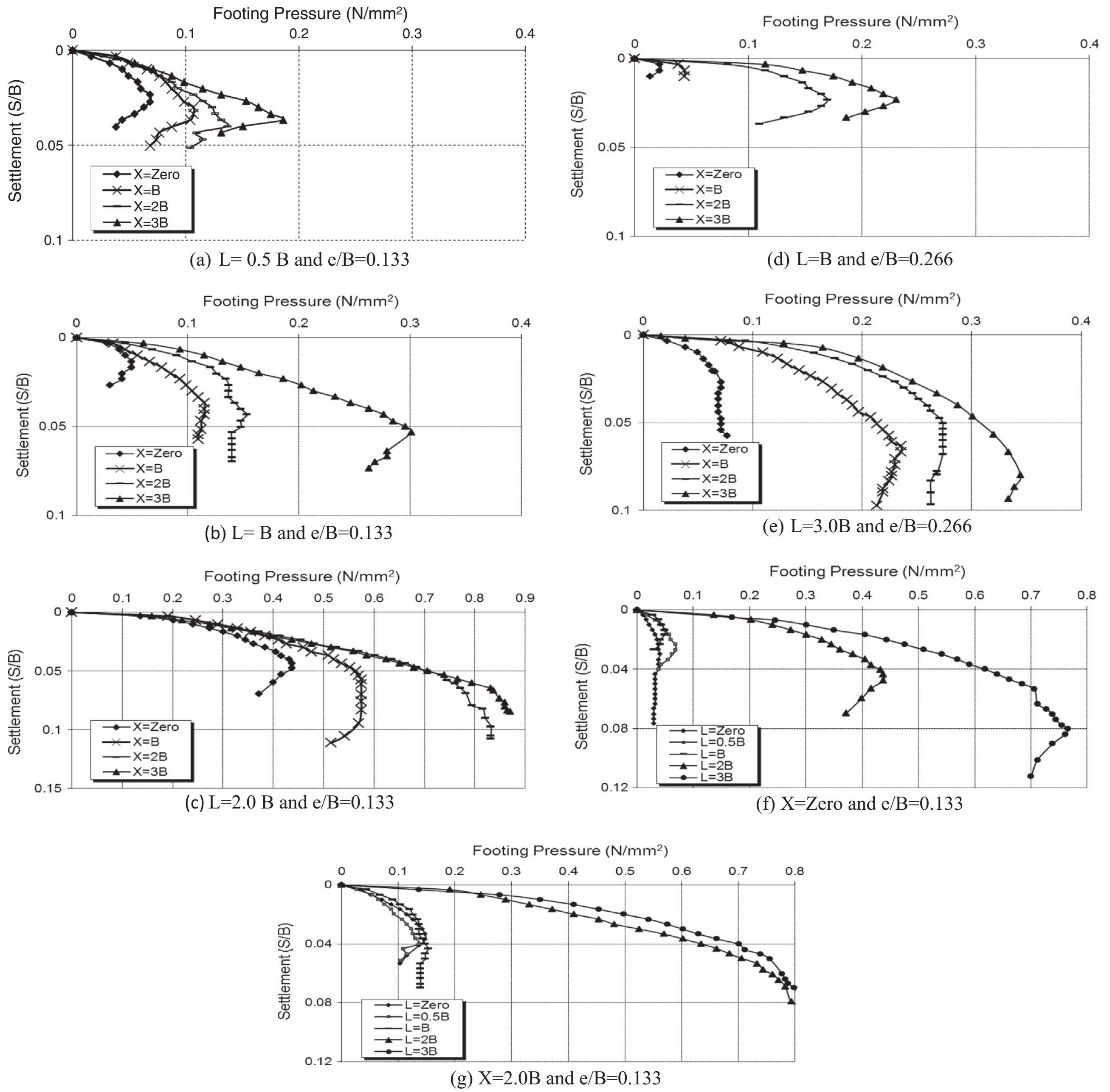

Figure 9 Load-settlement relations for eccentric loaded micro-piles footing on slope 3:2.

loading progress. This explained the small effect of the micro-piles that have a depth less than the slope height. The micro-piles having $L/B < 2.0$ provided only partial confinement to the surrounding soil. Small additional improvement in BCR_u was gained by increasing the micro-piles depth beyond the ratio $L/B = 2.0$. The amount of improvement in the ultimate bearing capacity ratio due to usage of micro-piles reached 7.9. In addition, the increase in micro-piles depth safeguarded the slope from excessive deformation and therefore postphones the collapse. The BCR_u decreased as the footing distance to the slope crest increased for footing loaded with eccentricity within the middle third and having L/B equal to 2.0 or more. This is due to increasing the footing distance to the slope crest that increased the confined soil which enhanced the footing stability. In contrary, it was observed that BCR_u for micro-piles footing loaded with eccentricity out of the middle third was not affected by footing position from slope crest.

5.3. Oblique loading

Footings subjected to centric oblique loads have two types of deformations; vertical and horizontal. The laboratory work was directed to study the behavior of single side micro-piles strip footing subjected to centrically oblique load ($i = 10°$). Samples of the load-settlement curves of the single side micro-piles strip footing tests resting on the top of sand slope (3:2) are drawn in Figs. 11 and 13. This was associated with the corresponding load and horizontal displacement relationship; Figs. 12 and 14. The failure load could be registered at the

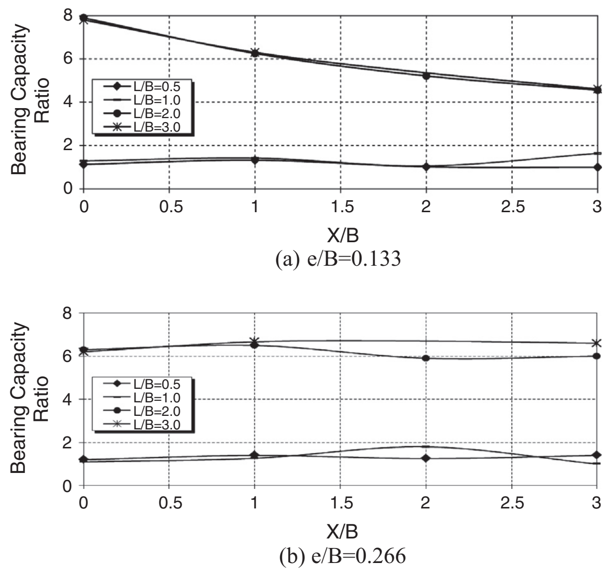

Figure 10 Ultimate bearing capacity ratio improvements.

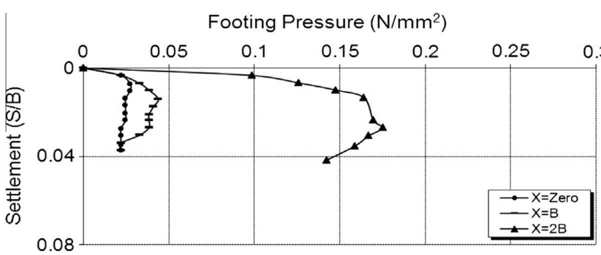

Figure 11 Load-settlement relation for micro-piles footing ($L = B$) subjected to oblique load ($i = 10°$) on slope 3:2.

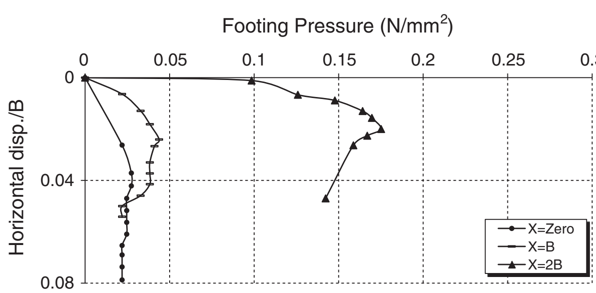

Figure 12 Load-horizontal displacement relation for micro-piles footing ($L = B$) subjected to oblique load ($i = 10°$) on slope 3:2.

point of failure or when the footing started to slide horizontally. The cohesionless soil particles under the footing subjected to centric inclined load tend to move laterally in the direction of the applied load. The footing was forced to tilt and slide at the same time. Therefore, the increase in footing tilt leads to an increase in the horizontal component of the inclined load which forces the footing to slide. The micro-piles resist the footing tilting caused by the inclined load resulting in bearing capacity improvement. The sliding stability is considered one of the critical factors when dealing with the overall stability of footing subjected to inclined load. Construction of micro-piles beneath the footing generates a passive pressure

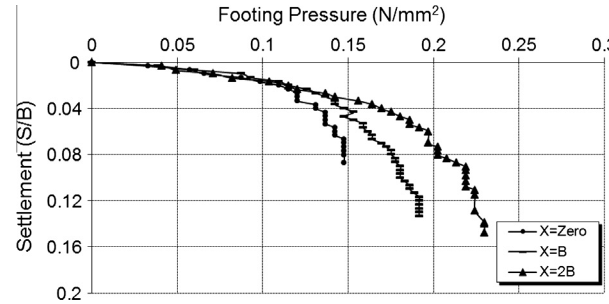

Figure 13 Load-settlement relation for micro-piles footing ($L = 4.0\ B$) Subjected to oblique load ($i = 10°$) on slope 3:2.

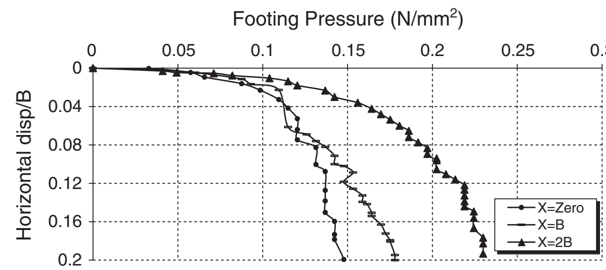

Figure 14 Load-horizontal displacement relation for micro-piles footing ($L = 4.0\ B$) subjected to oblique load ($i = 10°$) on slope 3:2.

on the micro-piles which enhances the footing to resist sliding. Results indicate that increasing the micro-piles depth leads to an increase in the footing pressure at the same settlement level. This could be mainly due to the increased in the volume of the laterally displaced soil that induced an improvement in the soil resistance on the micro-piles sides. The gabs between the micro-piles prevented the soil to pass through the micro-piles due to soil arch actions. This results in compacting sand in the front of the micro-piles. Consequently, it generates a high resistance to the horizontal displacement of the footing. In order to resist the horizontal forces, a horizontal displacement should take place. This displacement was found to vary considerably according to the micro-piles depth. The amount of improvement in the BCR_u value, due to the presence of micro-piles depth up to $L/B = 4.0$, is 4.5. Furthermore, the horizontal displacement was reduced by about 300% due to the micro-piles effect.

6. Conclusions

Based on the experimental results and analysis carried out on one sided micro-piles strip footing located on or adjacent to dense sand slope, the following conclusions can be drawn:

- Increasing the distance between the footing edge and the slope crest leads to increasing the bearing capacity. Beyond a distance of about five times the footing width, away from the slope crest, the influence of the slope becomes negligible on the bearing capacity of footing. Most of bearing capacity increment occurs at X/B of 0.0 to 2.0.
- The bearing capacity is considerably increased and the ground settlement is also decreased due to installation of single side micro-piles on strip footings.

- The bearing capacity is increased with increasing the micro-piles depth and reaches its maximum when the micro-piles rest on the stable soil just beneath the slope bed.
- The enhancement of BCR_u occurs simultaneously with the increment of micro-piles depth to reach in some cases about 7.9 times the footing without micro-piles.
- Insertion of single side micro-piles in strip footing subjected to concentric vertical loads is not recommended for micro-piles depth up to the footing width.
- The BCR_u is decreased as the footing distance to the slope crest is increased for footing loaded with eccentricity within the middle third and having L/B equal to 2.0 or more. The BCR_u has no variation, due to footing position. This occurred for micro-piles footing loaded with eccentricity out of the middle third.
- The micro-piles could resist the footing tilting and sliding caused by the inclined load due to bearing capacity improvement. The horizontal footing displacement is reduced by about 300% due to the presence of the micro-piles effect.

References

[1] G.G. Meyerhof, The ultimate bearing capacity of foundations on slopes, in: Proceedings of the 4th International Conference on Soil Mechanics and Foundation Engineering, vol. 1, Div. 1–3a, 1957, pp. 384–386.

[2] J. Graham, M. Andrews, D.H. Shields, Stress characteristics for shallow footings in cohesionless slopes, Can. Geotech. J. 25 (2) (1988) 238–249.

[3] S. Saran, V.K. Sud, S.C. Handa, Bearing capacity of footings adjacent to slopes, J. Geotech. Eng., ASCE 115 (4) (1989) 553–573.

[4] A.K. Nazier, The Bearing Capacity of Strip Footings Resting on Sand Adjacent to a Slope with the Presence of a Horizontal Flat Rigid Boundary, M.Sc. Thesis, Civil Engineering Department, Cairo University, Cairo, Egypt, 1996, pp. 135.

[5] O. Kusakabe, T. Kimura, H. Yamaguchi, Bearing capacity of slopes under strip loads on the top surfaces, J. Soils Found. 21 (4) (1981) 29–40.

[6] D.H. Shields, N. Chandler, J. Garnier, Bearing capacity of foundations in slopes, J. Geotech. Eng., ASCE 116 (3) (1990) 528–537.

[7] P. Arduino, E.J. Macari, M. Gemperline, Load-settlement prediction of footings on steep slopes, in: Proceedings of the Conference on Vertical and Horizontal Deformations of Foundations and Embankments, USA, Publ. by ASCE, vol. 2, 1994, pp. 1385–1399.

[8] M.C. Gemperline, H.Y. Ko, Centrifugal model tests for ultimate bearing capacity of footings on steep slopes in cohesionless soils, in: Proceedings of a Symposium on the Application of Centrifuge Modeling to Geotechnical Design, Manchester, England, 1985, pp. 203–221.

[9] J.I. Clark, S. Mckeown, C.B. Crawford, Field measurements of the behavior of inclined footings on a natural slope, Can. Geotech. J. 25 (4) (1988) 662–674.

[10] G.E. Bauer, Bearing capacity of footings in granular slopes, in: Proceedings of the 11th International Conference on Soil Mechanics and Foundation Engineering, Balkema, Rotterdam, the Netherlands, vol. 2, 1981, pp. 33–36.

[11] A.P. Soriano, M.C. Valderrama, J.G. Gonzalez, Bearing capacity of shallow foundations on sloping ground, in: Proceedings of the 15th International Conference on Soil Mechanics And Geotechnical Engineering, Istanbul, vol. 1, 2001, pp. 773–776.

[12] C.C. Huang, F. Tatsuoka, Y. Sato, Failure mechanisms of reinforced sand slopes loaded with a footing, J. Soils Found. 34 (2) (1994) 27–40.

[13] K.M. Lee, V.R. Manjunath, Experimental and numerical studies of geosynthetic-reinforced sand slopes loaded with a footing, Can. Geotech. J. 37 (4) (2000) 828–842.

[14] G.L. Babu, B. Murthy, M.S. Nataraj, Bearing capacity improvement using micro-piles: a case study, in: Proceedings, Geosupport Conference, 2004, pp. 692–699.

[15] J. Han, S.L. Ye, A field study on the behavior of a foundation underpinned by micro-piles, Can. Geotech. J. 43 (1) (2006) 30–42.

[16] A. Bhattacharjee, S. Mittal, A.M. Krishna, Bearing capacity improvement of square footing by micro-piles, Int. J. Geotech. Eng. 5 (1) (2011) 113.

[17] I. Juran, D.A. Bruce, A. Dimillio, A. Benslimane, Micro-piles: the state of practice. Part II: Design of single micro-piles and groups and networks of micro-piles, J. Ground Improve. 3 (1999) 89–110.

[18] G. Russo, Full-scale load tests on instrumented micro-piles, Geotech. Eng. J. 157 (3) (2004) 127–135.

[19] W. Armin, D. Matt, E. Garry, Tension and compression micropile load tests in gravelly sand, in: 6th International Conference on Case Histories in Geotechnical Engineering, Arlington, VA, August, 2008, pp. 11–16.

[20] N. Pinyol, E. Alonso, Design of micro-piles for tunnel face reinforcement: undrained upper bound solution, J. Geotech. Geoenviron. Eng. 138 (1) (2012) 89–99.